Simulating Extrasolar Planet Populations for Direct Imaging Surveys

Eric L. Nielsen[1]†, L. M. Close[1] and B. A. Biller[1]

[1]Steward Observatory, University of Arizona, Tucson, AZ 85721, USA
email: enielsen@as.arizona.edu

Abstract. As high contrast imaging surveys are being designed and carried out to directly detect extrasolar planets around young, nearby stars it is important to carefully evaluate the criteria for selection of target stars, as well as the predicted success of such a survey based on the sensitivity of the AO system used. We have developed a routine to simulate a large number of planets around each potential target star, and determine what fraction can be reliably (5σ) detected using an AO system's predicted or observed sensitivity curve (the maximum flux ratio between the parent star and a detectable planet as a function of projected radius). Each planet has a randomly assigned semi-major axis, mass, and eccentricity (following extrapolations of detected radial velocity planet power laws), as well as random viewing angles and orbital phase. The orbital parameters give a projected separation for each planet, while the mass is converted into a flux ratio in the appropriate bandpass of the detector using the models of Burrows *et al.* (2003); this allows the simulated planets to be directly evaluated against the system's sensitivity curve. Since this method requires basic parameters (age, distance, spectral type, apparent magnitude) for each target star, a target list can be constructed that maximizes the likelihood of detecting planets, or competing instrument designs can be evaluated with respect to their predicted success for a given survey. We are already employing this method to select targets for our Simultaneous Differential Imaging (SDI) surveys (Biller *et al.* 2004), now underway at telescopes in the northern (MMT) and southern hemispheres (VLT).

Keywords. Stars: Planetary Systems, Techniques: High Angular Resolution.

---

1. Introduction

With the number of detected extrasolar planets continuing to climb well over one hundred, astronomers are finally in a position to begin to characterize the process of planet formation, as well as give statistical descriptions of planet populations around nearby stars. A significant gap, however, exists in our knowledge for planets with orbits at or beyond that of Jupiter: the widest orbit known for a confirmed extrasolar planet is 6 AU, for 55 Cnc d (Marcy *et al.* 2002). Since this limit is set by the time baseline of radial velocity surveys, this threshold will march out slowly; it will take another 15 years to close an orbit equivalent to Saturn's (9.5 AU). Radial velocity detections of planets in this regime will be further hampered by the fact that the amplitude of the velocity declines with the inverse square root of the semi-major axis.

Direct imaging, then, serves as a completely complimentary detection method to radial velocity surveys, as it is most sensitive to planets with large separations from their parent stars, with no real upper limit to detectable semi-major axes. If the two techniques could be brought together at intermediate separations, we will be able to start building up a complete picture of the distribution of planets. Again, since radial velocity surveys are slow to move outward, direct imaging is well-situated to close the gap.

† Michelson Fellow

SDI, or Simultaneous Differential Imaging, is a technique to achieve very high contrast images at small angular separations. By obtaining images simultaneously through narrow-band filters centered on either side of the 1.6 μm methane bandhead, we can greatly attenuate speckle noise from the star, and achieve very high contrasts for objects with a strong methane signature (most giant planets). We are currently conducting a survey for planets around young, nearby stars using SDI cameras installed at the VLT and MMT. For further information on SDI and the progress of our survey, see Lenzen *et al.* 2004 and Biller *et al.* 2004, as well as the contributions to this proceedings by B. Biller and L. Close.

2. Monte Carlo Simulations

The ability of a survey instrument to detect self-luminous, giant extrasolar planets is typically given in the form of a contrast curve: the faintest magnitude (expressed in relation to the magnitude of the parent star) at which a companion can be significantly detected, given as a function of the angular separation between the two objects. We have assembled a set of four sensitivity curves in order to illustrate the nature of our simulations, as shown in Fig. 1. VLT NACO SDI represents a currently available system, on the 8.2m VLT telescope with a 200 element Shack-Hartmann wavefront sensor, using four-channel SDI optics to reduce speckle noise (Lenzen *et al.* 2004, Biller *et al.* 2004, contrast curve from B. Biller *et al.*, this proceeding). Gemini NICI is expected to come on-line by 2006, utilizing the H85 AO systems, an 85 element curvature wavefront sensor, along with a coronograph and two-channel SDI optics (predicted sensitivity curve from the NICI Request for Proposal (2005)). We also include plausible contrast curves for Extreme Adaptive Optics Coronographs (ExAOC) at an 8m-class telescope, or at the proposed 24m Giant Magellan Telescope (Johns *et al.* (2004)). In either case, our curves consist of a spatially-filtered Shack-Hartmann wavefront sensor (750 element for the 8m telescope, 4400 for the GMT), a coronograph, a focal-plane wavefront sensor for speckle suppression (Codona and Angel (2004)), and SDI optics for added contrasts (Codona *et al.* (2005)).
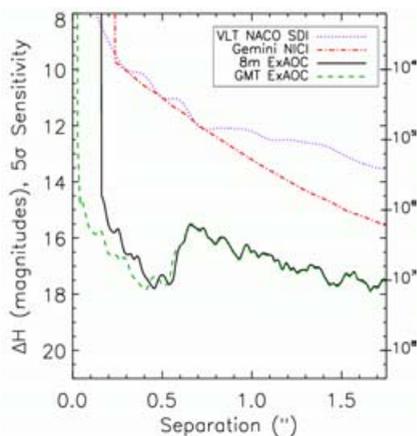
Figure 1. Sensitivity curves for the four planet-finding instruments we consider here. The curves represent the 5σ level of detection for a companion at a given angular distance from the parent star, after an integration of 10,000 seconds.

While the contrast curves of Fig. 1 describe the comparative abilities to image faint companions of the four systems, it is not immediately apparent how these curves translate into the figure of merit about which we're most concerned: the number of planets each system could detect from a survey. In order to evaluate this, we have constructed a Monte-Carlo simulation to create an ensemble of planets, compute their projected separation
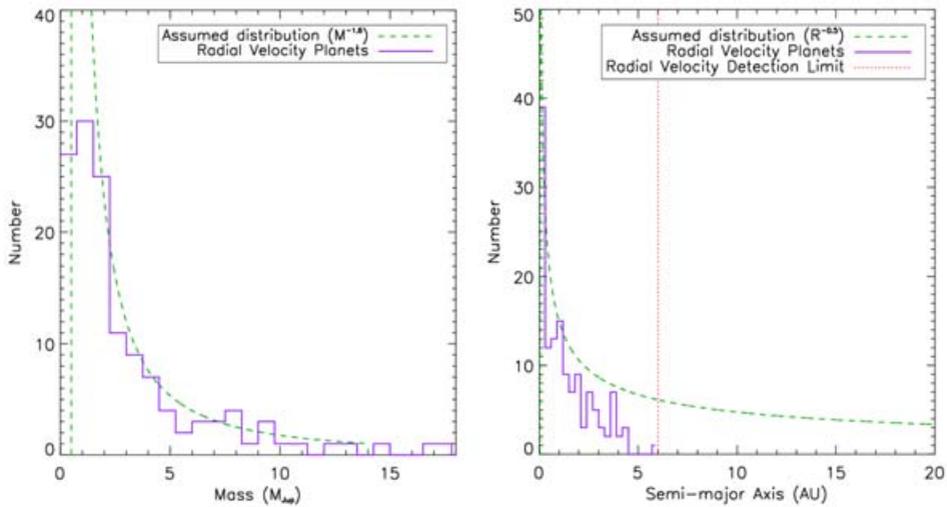
Figure 2. The assumed distributions of mass (power law index -1.6) and semi-major axis (-0.5) of extrasolar giant planets, plotted against histograms of known planets from radial velocity surveys.

and H-magnitude, then compare them to these contrast curves to determine what fraction can be detected with a given system.

For each target star we simulate 100,000 planets, randomly generating six quantities for each planet: mass, semi-major axis, eccentricity, inclination angle, longitude of periastron, and orbital phase. Mass and semi-major axis are assumed to be governed by simple power-law distributions, with indices chosen to fit the population of known radial velocity planets, as shown in Fig. 2 (similar distributions were inferred by Lineweaver and Grether (2003) for mass and Graham *et al.* (2002) for semi-major axis). Distributions of extrasolar planets are taken from California & Carnegie Planet Search Almanac of Planets (2005). High and low mass cut-offs are imposed on the power law distribution at 0.5 and $14\,\mathrm{M}_{Jup}$, and the semi-major axis distribution is truncated at 0.037 AU (orbital radius of the innermost known extrasolar planet, HD 73256) and 20 AU. This outer limit for semi-major axis is uncertain, as the data from extrasolar planet surveys become incomplete beyond ∼3 AU, and no data exist for extrasolar planets further out than 6 AU. We take 20 AU (the orbit of Uranus) as a conservative upper limit. The distribution for eccentricity is taken as a simple polynomial fit to the histogram of eccentricities of radial velocity planets.

It should be noted that we have assumed three independent distributions for mass, semi-major axis, and eccentricity of planets, which is almost certainly incorrect. With only 137 known planets, however, the statistics are not sufficient to suggest a more complex distribution. For this same reason, we also assume these planet distributions to be independent of the spectral type of the parent star.

We also assign an inclination angle for the orbit (uniform in cos(i)), longitude of periastron (uniform between 0 and 2π), and orbital phase (uniform random variable is time; between 0 and 1 orbital periods). From these six quantities we can solve for the instantaneous separation between planet and star, as viewed from the observer on earth. The distance to the target star can then be used to solve for angular separation. With the planet models of Burrows *et al.* (2003), the planet's mass (along with the age of the target star) is converted into an H-magnitude, which we use to solve for ΔH, given the
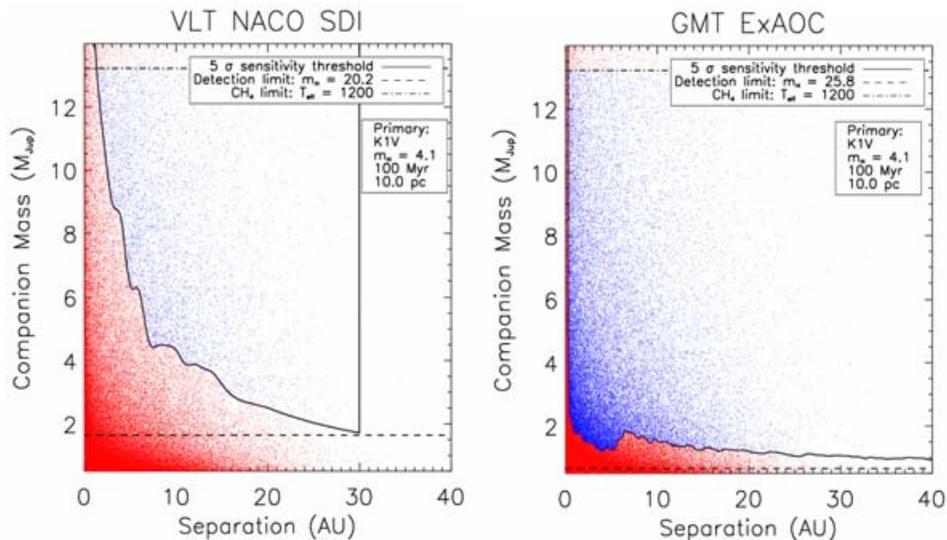
Figure 3. Example simulations for a particular target star with the VLT NACO SDI (left) and GMT ExAOC (right) systems. Each point represents a single simulated planet, out of a total of 100,000 in the simulation run. Detected planets lie above the 5σ sensitivity curve (solid line) and the detection threshold (bottom dashed line), and below the methane limit (top dotted line). For VLT NACO SDI, 6% of these planets are detected; GMT ExAOC can detect 35%.

distance and 2MASS flux of the target star. Then, it is determined whether or not each planet can be detected, given the sensitivity curve of Fig. 1.

We show examples of these simulations for a single target star in Fig. 3. In addition to the sensitivity limit, we consider if the apparent magnitude of the planet is sufficient to be detected by photon noise arguments alone, and whether the planet is too massive (hence too hot) to have a significant methane feature (SDI is most effective when there is a strong drop in the planet's spectrum at the methane bandhead, $T_{eff} < 1200$K). We can now directly compare two systems by their ability to find planets: VLT NACO SDI should have a 6% chance of finding a planet around the star in Fig. 3, while GMT ExAOC will be at 35%.

3. Target Selection

The ideal target star for a direct imaging survey for self-luminous extrasolar planets is characterized by three traits: the star should be young so the planet's luminosity is larger, the star should be nearby so the angular separation between primary and companion is greater, and the star should be of a late spectral type so that the inherent luminosity of the star does not overwhelm the planet's light. It is not trivial to find a balance between these factors to select an observing list for a survey. In particular, there is a lack of very young stars (<30 Myr) very close (<20 pc) to the sun (especially in the northern sky), so compromises must be made. It is through the simulations described in this paper that we seek to disentangle these target star traits, so that every potential target gets a quantitative ranking. By constructing a survey that maximizes the expected number of planets detected, our results (even null results) become more meaningful.

Another important consideration (especially for higher-order AO systems such as ExAOC) is the limiting magnitude at which the adaptive optics can efficiently operate. Better sampled AO systems (more wavefront measurements, and more actuators to

control) require more photons from the guide star, with strehl ratios (and so contrasts) declining faster for fainter guide stars. Since our simulations indicate a preference for younger, further-out stars over older, nearby targets, a planet-finding system with a limiting magnitude that is too bright will exclude many of the best targets. For example, of the 40 best targets from our list of 153 (which we have compiled from the literature), the median V magnitude is 9.75; a next-generation AO system that can't lock onto targets fainter than 9th magnitude will simply not be an efficient planet finder, as half the potential targets are eliminated before the survey begins. This effect can be mitigated by allowing the AO system's performance to be modulated depending on the target star (having the wavefront sensor integrate longer on fainter stars, for example), at the expense of contrasts. In any event, when designing future adaptive optics systems with the primary goal of detecting extrasolar planets, one must be keenly aware of the nature of the available science targets when evaluating potential instrument designs. The number of target stars for direct imaging surveys for self-luminous extrasolar planets is limited, and an instrument that cannot reach most of them would not be competitive.

4. Simulation Results

We now consider the implications of our simulation results for the selection of target stars. In Fig. 4 we examine the fraction of planets that can be detected around target stars of various ages and distances. As expected, younger, nearby targets are more likely to harbor detectable planets. The probability of detecting a planet around an older, or more distant, star drops quickly. We also look at results of the simulation for all 153 of our target stars, plotting the median separation of the detected planets (See Fig. 3) against the percentage of planets that are detectable. The more sophisticated planet-finding systems are more powerful since they minimize the inner working radius, as we would expect most planets to lie at small angular separations from their parent stars.

We also consider the predicted results of a planet-search campaign, directed at our target list, using the four systems. Since the simulations return the probability of detecting a planet around a given star, the sum of these probabilities for all the survey stars should give us the total number of planets we'd expect to detect at the end of a survey. In Fig. 5 we have ordered our targets by detection probability (so the highest-quality targets are observed first), and show the expected yield of planets from surveys of various sizes. Clearly, most of the planets are found initially, as the best targets are observed, and adding lesser-quality target stars to the observing campaign results in a slower gain in planets. The break in these curves, between rapid return of planets and a more gradual increase, depends on the nature of the instrument.

5. Conclusions

With these simple Monte Carlo simulations, extrapolating from populations of known extrasolar planets, we have a method to quantitatively rank stars in a target list for a planet search campaign, or to directly compare competing instrument designs for future planet finding systems. Our basic results suggest that there are a limited number of target stars suitable for direct imaging searches for self-luminous planets, a fact that must be considered when planning a survey or designing a new instrument.

Finally, we consider one of our basic assumptions: that each of our target stars has one planet described by the power laws of Fig. 2. While there is a lack of data for planet populations at large separations, we can make an estimate of total populations based on our initial assumptions and results from radial velocity surveys. Fischer and Valenti
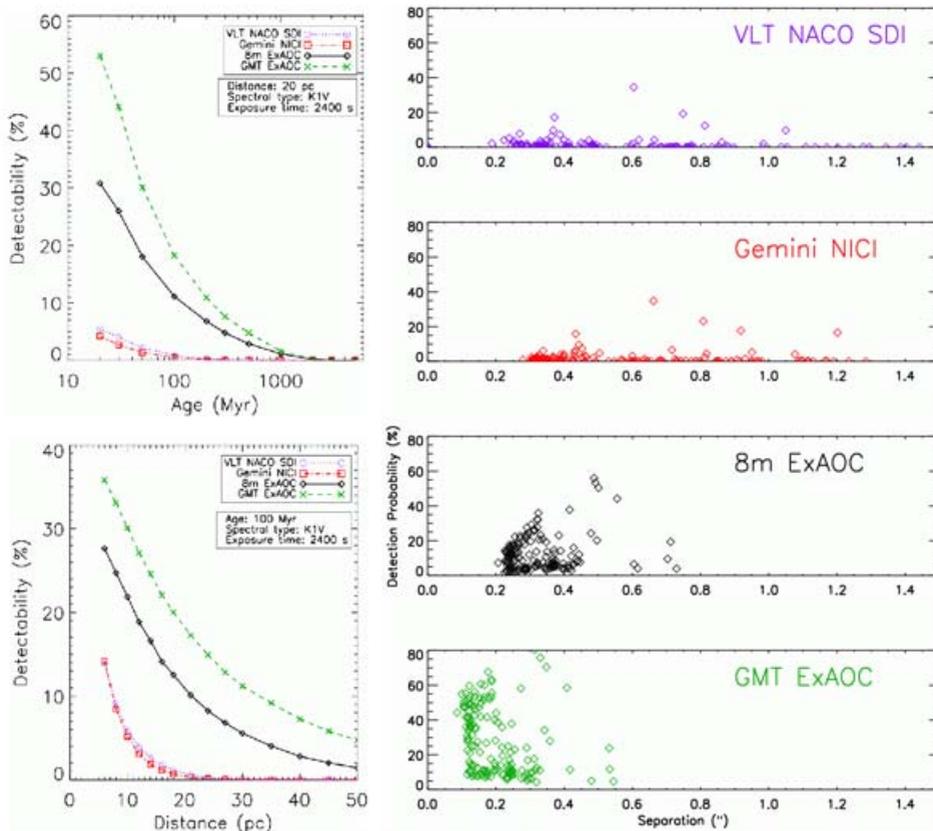
Figure 4. Basic results from the simulation. Top left shows the fraction of simulated planets detected (the detection probability) for target stars of different ages. As expected, younger stars are the preferred targets for finding self-luminous planets, and there is very little value in observing older (>1 Gyr) target stars. Bottom left is a similar plot, only with distance being varied. In the right panel, we consider the properties of the simulated planets that can be detected with each system. For each of the 153 target stars, we plot the fraction of planets that can be detected (y-axis) against the median projected separation (in arcseconds) between primary and companion for those planets that can be detected. The pile-up at small separations underscores the critical importance of the inner working radius of any planet-finding system.

(2005) determine that in a volume-limited sample, about 6% of stars show the radial velocity signature of a massive planet with an orbital period shorter than 4 years (2.5 AU for a solar mass primary). Given this, we can then integrate our assumed semi-major axis distribution ($dN/da = a^{-0.5}$), to give the total number of planets between 0.03 and 20 AU (which we simulate), compared to the fraction found by Fischer and Valenti (2005) between 0.03 and 2.5 AU. From this argument, we'd expect 18% of all stars to have a giant planet, or 40% for stars of solar metallicity or greater. This simplistic argument does not take into account possible effects of changing planet populations (or overall frequency) with spectral type of the parent star, an issue that is still being studied. Nevertheless, as these simulations make real predictions about survey results, they place us in a strong position to interpret any results as they relate to the overall populations of extrasolar planets.
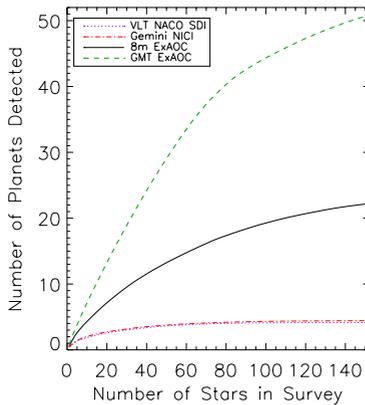
Figure 5. The number of planets expected to be detected, as a function of the number of stars in the survey. In each case, once the best targets are observed, there is a slow gain in planets detected as lower-quality targets are added to the survey. The location of this break, however, depends on the ability of the instrument (in order of increasing power: VLT NACO SDI and Gemini NICI, 8m ExAOC, and GMT ExAOC).

References

Biller, B.A., Close, L., Lenzen, R., Brandner, W., McCarthy, D.W., Nielsen, E. & Hartung, M. 2004, *SPIE* 5490, 389

Brown, R.A. 2004, *ApJ* 607, 1003

Burrows, A., Sudarsky, D. & Lunine, J.I. 2003, *ApJ* 596, 587

California & Carnegie Planet Search Almanac of Extrasolar Planets 2005

Codona, J.L. & Angel, R. 2004, *ApJ* 604, 117

Codona, J.L., Angel, R., Close, L. & Potter, D. 2005, private communication

Fischer, D.A. & Valenti, J. 2005, *ApJ* 622, 1102

Graham, J.R., Macintosh, B., Ghez, A., Kalas, P., Lloyd, J., Makidon, R., Olivier, S., Patience, J., Perrin, M., Poyneer, L., Severson, S., Sheinis, A., Sivaramakrishnan, A., Troy, M., Wallace, J. & Wilhelmsen, J. 2002, *AAS* 201, 2102

Johns, M., Angel J.R.P., Schectman, S., Bernstein, R., Fabricant, D.G., McCarthy, P. & Phillips, M. 2004, *SPIE* 5489, 441

Lenzen, R., Close, L., Brandner, W., Biller, B. & Hartung, M. 2004, *SPIE* 5492, 970

Lineweaver, C.H. & Grether, D. 2003, *ApJ* 598, 1350

Marcy, G.W., Butler, R.P., Fischer, D.A., Laughlin, G., Vogt, S.S., Henry, G.W. & Poubaix, D. 2002, *ApJ* 581, 1375

NICI Planet Finding Campaign, Request for Proposals 2005

Discussion

QUESTION: Doesn't the conclusion that inner working angle is the most important aspect of the system depend heavily on your choice of distribution for semi-major axis?

NIELSEN: Yes, an alternate distribution with a reservoir of giant planets at large separation would result in less importance being assigned to the inner working angle. We have sought to take a conservative approach, extrapolating only from the known radial velocity planets which suggest, even given the observational biases, a declining frequency of planets with semi-major axis. Though not conclusive, the lack of planets found thus far by current direct-imaging surveys, especially in the large separation regime in which

they are most sensitive, suggests that a large semi-major axis reservoir of planets does not exist past 50 AU.

QUESTION: Wouldn't your concern about guide star magnitude go away if a laser guide star system were used?

NIELSEN: For the case of ExAOC, for both the 8m and 24m telescopes, laser guide stars would not be competitive with natural guide stars. The goal of Extreme Adaptive Optics is to achieve strehls >90%, which is not achievable at H-band with a laser system. A sodium laser guide star would be 90 km above the telescope, with the science target at essentially infinity. Both make a cone with the point source at the tip and telescope's primary mirror at the base. If there is a turbulent layer 10 km above the telescope, the cone of the star (basically a cylinder through the atmosphere) would be larger than that of the Na laser beacon's by about 20%: this is turbulence that distorts the wavefront of the science target, which the laser beacon's light never samples. This so-called "cone" effect alone precludes lasers from being a part of an ExAOC system, as typical strehls achieved with lasers are <50% at H-band.